Evaluation of the chemical and optical perturbations induced by Ar plasma on InP surface

Solène Béchu, Céline Eypert, Anais Loubat, Jackie Vigneron, Sofia Gaiaschi, Patrick Chapon, Muriel Bouttemy, Arnaud Etcheberry

Evaluation of the chemical and optical perturbations induced by Ar plasma on InP surface

Solène Béchu[1,2,a)], Céline Eypert[3], Anais Loubat[2], Jackie Vigneron[2], Sofia Gaiaschi[3], Patrick Chapon[3], Muriel Bouttemy[2], Arnaud Etcheberry[2]

[1] *Institut Photovoltaïque d'Ile-de-France (IPVF), 18 Boulevard Thomas Gobert, 91120 Palaiseau, France.*
[2] *Institut Lavoisier de Versailles (ILV), Université de Versailles Saint-Quentin-en-Yvelines, Université Paris Saclay, CNRS, 45 avenue des Etats-Unis, 78035 Versailles, France,*
[3] *HORIBA Scientific, 14 Boulevard Thomas Gobert, Passage Jobin Yvon, CS 45002, 91120 Palaiseau, France*
[a)] Electronic mail: solene.bechu@uvsq.fr

Abstract

Interfaces are of primary importance in heterostructures. We propose here an innovative methodologic development to access the chemical information in depth and, more especially, at buried interfaces. This specific approach is based on the combination of Glow Discharge Optical Emission Spectroscopy (GD-OES) plasma profiling, enabling to quickly and precisely reach buried interfaces, with X-Ray Photoelectron Spectroscopy surface analyses, bringing an accurate determination of the composition and the chemical environments. The representativeness of the crater chemistry is therefore a critical issue. On InP substrate, the fine examination inside the GD-OES crater reveals surface modifications, both chemical, morphological and optical, and as a consequence the need to regenerate the initial chemical information. We present here a study dedicated to the evaluation of those modifications thanks to a multi-technique approach, with an important contribution of Spectroscopic Ellipsometry measurements. A crater regeneration strategy, by means of a nano-chemical etching, is proposed and also assessed by the same analytical pathway, proving the recovery of the initial InP properties.

I. INTRODUCTION

Access to the chemistry of buried interfaces is a key parameter in the comprehension of heterostructures properties and can be reached through a lot of different experimental techniques[1–3]. Recently we developed a combination of Glow Discharge-Optical Emission Spectrometry (GD-OES) depth profiling and X-Ray Photoelectron Spectroscopy (XPS) surface characterization[4] to precisely determine the chemistry at interfaces buried at several micrometers, in a reasonable acquisition time. GD-OES profiling is used as a very efficient and quantitative method (after intensities calibration on standards) to determine atomic concentration profiles of thin films stacks. When arriving close to a critical interface, GD-OES can be stopped and relayed inside the etched crater by a sequential XPS analysis, assisted or not with Ar or Ar_n^+ ion profiling in order to be as close as possible to the interface thanks to XPS profiling. This analytical strategy strongly refines the chemical profile accuracy on both sides of interfaces of interest as it additionally brings the direct atomic composition and the chemical environment information in the same experimental sequence[4]. This combination is therefore particularly well adapted to perform an efficient and complete characterization of heterostructures. Nevertheless, a main question relative to this GD-OES/XPS coupled approach concerns the integrity of the information inside the GD-OES crater, which condition the representativeness of the XPS interpretation of the chemistry at buried interfaces. Thus, a systematic control of the crater surface physico-chemical properties is necessary to ensure the reliability of the relay between GD-OES and XPS. Surface modifications observed when stopping the plasma etching differ with the nature of the material. Therefore they have to be considered case by case to determine, if necessary, the best physical or chemical procedure to recover the initial information. This knowledge is essential to further implement consistent GD-OES/XPS coupling and perform an advanced chemical characterization of more complex blocks such as heterostructures.

To evaluate the modifications inside the GD-OES crater, a multi-technique approach is employed to determine the chemical (XPS, Energy-Dispersive X-Ray Spectroscopy –EDS-), morphological (Scanning Electron Microscopy –SEM-), microstructural (Electron Back-Scattering Diffraction –EBSD-) and optical Spectroscopic Ellipsometry (SE) characteristics of the surface and sub-surface. Among this set of techniques, SE is less usually employed for such a study and we will emphasize its added value. SE represents an efficient nondestructive characterization method, particularly well adapted to material surfaces and thin films analyses[5]. SE is a perfect optical tool to detect even slight surface evolutions, due to different kinds of perturbations. Indeed, SE can be used to qualitatively detect evidences of plasma induced modifications and the subsequent effect of the chemical engineering necessary to remove the perturbed surface layer, therefore enabling the step by step[6,7] monitoring of the surface evolutions. Moreover, through an adapted modeling step, it provides quantitative optical data linked to such modifications. The optical SE responses also allows an autonomous diagnosis directly related to chemical features[5]. However the determination of perfect surface optical parameters needs some physical constraints, as for example minimal surface roughness[8]. Semi-quantitative or quantitative SE interpretation will then depend on the morphological consideration onto the surface.

The present work focuses on the evaluation of the GD-OES crater perturbation on one specific III-V material: InP. Evolutions of optical parameters are determined with SE, directly implemented in the crater, just after GD-OES profiling stop (corresponding to the XPS relay step in our GD-OES/XPS combined approach) as well as after wet chemical treatments dedicated to the GD-OES crater regeneration. InP is one of the most studied III-Vs semi-conductor, especially under reactive conditions[9], and its SE response has been largely described in many different situations on well-defined surfaces[10–14]. Providing quantitative information about the GD-OES crater impact is therefore a very interesting challenge for SE.

The SE goal is to inform about the possible modifications induced by the plasma etching, their nature and, if possible, the amount of external material impacted by such modifications. SE measurements combined with XPS characterization inside the crater could provide a quantitative description of the perturbations induced or not (stoichiometry, surface oxidation, effective perturbed depth, presence of post etching film, etc). The use of other easier characterizations techniques (SEM, EDS, EBSD) is also an important purpose to completely understand the perturbation nature. The robustness of this multi-technique approach will be discussed and particularly the autonomy of the SE as an efficient probe to show the perturbation induced by the plasma etching. After the initial crater examination, the question of the crater bottom recovery is detailed. The efficiency of wet chemical engineering is studied and again the capability of SE to demonstrate that the crater cleaning is effective is demonstrated.

II. EXPERIMENTAL

GD-OES experiments are performed using a pulsed RF glow discharge optical emission spectroscopy (GD-PROFILER 2, HORIBA Scientific) equipped with the DiP (Differential Interferometry Profiling). Samples are sputtered with a pulsed Ar plasma up to 120 seconds according to the following parameters: 650 Pa, 30 W and 3000 Hz. The DiP module gives access to a direct and continuous measurement of the crater depth during the GD-OES analysis (i.e. depth vs sputtering time) and allows to stop at specific depths. This accessory uses an interferometric method with a red laser diode at 633 nm (that generates no perturbation of the GD-OES analysis as there are no spectroscopic lines of interest in this spectral region) and measures the relative phase-shift between the crater and the surface close to the crater. For non-transparent materials, such phase shift can be directly linked to the crater [15].

XPS surface chemical analyses are carried out with a Thermo Electron K-Alpha^{+} spectrometer using a monochromatic Al-Kα X-Ray source (1486.6 eV). The X-Ray spot size is 400 µm. The Thermo Electron procedure was used to calibrate the K-Alpha^{+} spectrometer by using metallic Cu and Au samples internal references (Cu $2p_{3/2}$ at 932.6 eV and Au $4f_{7/2}$ at 84.0 eV). High energy resolution spectra are acquired using a Constant Analyzer Energy (CAE) mode 10 eV and 0.05 eV as energy step size. Data are processed using the Thermo Fisher Scientific Avantage© data system. XPS spectra are treated using a Shirley background subtraction and XPS compositions are deduced using the sensitivity factors and the inelastic mean-free paths from Avantage© library associated to the spectrometer and the corresponding transmission function.

Spectroscopic Ellipsometry measurements are performed using a Phase Modulated Spectroscopic Ellipsometer (UVISEL+, HORIBA Scientific) over the spectral range 0.6-6.5eV at an angle of incidence of 70°. Modelings are performed with DeltaPsi 2 software.

Secondary Electron micrographs (SEM), elemental (EDS) and microstructural (EBSD) analyses are performed using a JEOL JSM 7001F microscope with a patented "in-lens" Schottky Field Emission Gun (FEG) equipped with an OXFORD Aztec EDS-EBSD system. SEM and EDS imaging analyses are realized at 10 kV accelerating voltage and 10 mm working distance, EBSD at 5kV.

Auger characterizations are performed with a JEOL JAMP 9500F Auger nano-probe also equipped with a patented "in-lens" Schottky Field Emission Gun (FEG) and a hemispherical analyzer (HAS). Experiments are carried out at 20 kV, 10 nA, tilt 0° leading to 12-15 nm spot size, the maximal analyzed depth being inferior to 4-5 nm. Spectra are acquired with a spectral resolution dE/E=0.5%.

The micro photoluminescence (PL) measurements are performed using a confocal Raman Microscopy system (Xplora PLUS, HORIBA Scientific), using a laser diode at 532 nm (laser diameter of 0.72 µm, measurement time 1s) at ambient temperature.

All transfers between GD-OES and surface (XPS, AES, and SEM) measurements are performed in less than 5 min.

.

III. RESULTS AND DISCUSSION

A. Modifications induced by GD-OES

The main information achieved with GD-OES profiler are the in-depth profile of the different elements present inside the etched layer as well as the different positions of the interfaces when they are crossed during profiling of heterostructures. In present case, the sample is only constituted of bulk InP. The GD-OES profile performed on InP is displayed in Fig. 1. a. and shows an expected constant atomic ratio (In/P = 1), whatever the depth of the crater. Before reaching the sputtering stationary state, a specific transient zone is observed (several seconds at the beginning of the experiment) due to surface contamination.

Thanks to the DiP module, the sputtered depth is also accessible. Here, a quasi-linear relationship between the DiP thickness measurement and the plasma exposure time is measured, in agreement with a quasi-constant etching rate (Fig. 1. b.). Up to 10 µm of InP are profiled in 120 seconds. Using the DiP tool, the etching time can be converted in etched depth and the precise localization in depth of a buried interface is made easier.

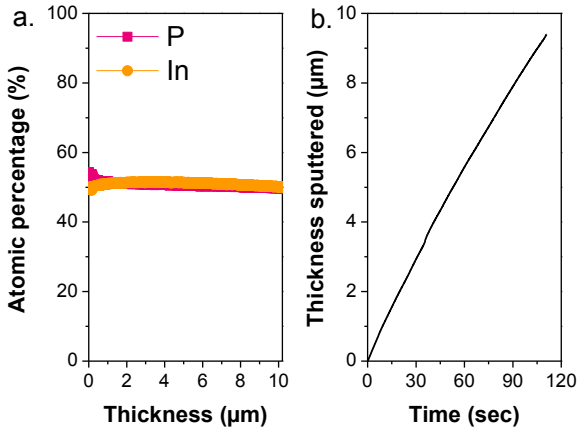

FIG. 1. GD-OES depth profile (atomic percentage vs thickness) for an InP layer (a.) and corresponding DiP measurement of the thickness sputtered over plasma exposure time (b.).

The main issue concerns now the surface state inside the GD-OES crater bottom. From previous studies on semi-conductors ($Cu(In,Ga)Se_2$, III-V binary compounds…)[4,16], we have shown that the plasma shut down is a critical step and leads to more or less significant chemical, optical and structural modifications, which depend on the nature of the layer. In the case of $Cu(In,Ga)Se_2$, when stopping the plasma sputtering, we have shown the presence of a superficial perturbed layer at the bottom crater both inherent to the plasma/material interaction (formation of metallic droplets, specific morphology…), the stop of the dynamic process (redeposition) and air exposure (oxidation). This overall examination of the crater surface is therefore imperative to determine if an intermediary step is required to eliminate this layer and access to the original chemical information by XPS.

1. Surface modifications

Comparing the physico-chemical properties of a pristine unexposed InP surface and the one obtained in the GD-OES crater is thus of primary importance. Modification of chemical environments as well as quantitative composition can be obtained through XPS measurements, which will serve here as a preliminary diagnosis tool.

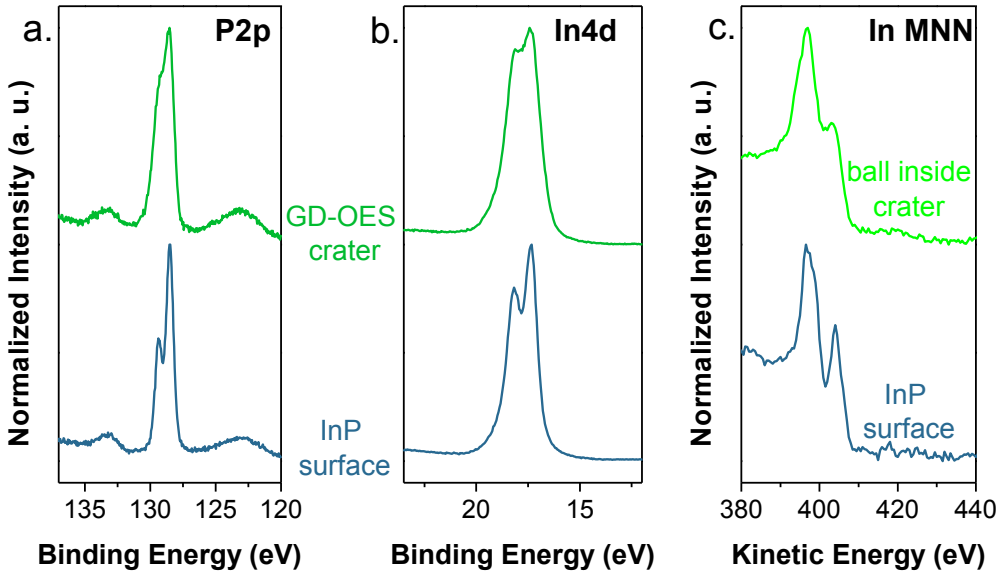

FIG. 2. XPS high energy resolution spectra of P2p (a.) and In4d (b.) photopeaks obtained on InP for an unperturbed surface (blue) and inside the GD-OES crater (green). Corresponding In MNN Auger transitions recorded at local scale using the Auger nano-probe outside (blue) and inside the crater (green) on specific features illustrated on Fig 3 b. and c.

Firstly, it has to be noted that no shift of the photopeaks energy position is visible either for P2p or for In4d (Table 1). On both spectra, oxide traces are present at a similar level as outside the crater, due to time transfer inside XPS analyses chamber. However, those traces are minimized regarding the InP surface, since the different oxide contributions start to grow after 30 minutes of air exposure. In metallic site presents a more critical reactivity. Indeed, In metal is very sensitive to air oxidation, but thanks to our fast transfer (less than 5 min air exposure), the surface modifications are thus minimized. Moreover, a large broadening of the Full Width at Half Maximum (FWHM) is visible (Table 1) for both photopeaks, increasing from 0.68 ± 0.05 to 0.96 ± 0.05 eV for In4d and 0.70 ± 0.05 to 1.02 ± 0.05 eV for P2p (spectra modelling not shown here). These FWHM enlargements are accompanied with the disappearance of the spin-orbit feature for both chemical elements (Fig. 2 a. and b.). These

modifications are typically observed when amorphization occurs, as already suggested for different bombardments[17] and other III-V materials[16].

TABLE 1. Evolution of the fitting parameters of In4d and P2p photopeaks.

Photopeaks	InP surface		GD-OES crater	
	BE (eV)	FWHM (eV)	BE (eV)	FWHM (eV)
$In4d_{5/2}$ - InP	17.3	0.68	17.4	0.96
$In4d_{3/2}$ - InP	18.2	0.68	18.3	0.96
$In4d_{5/2}$ - InP_{ox}	19.1	0.68	19.0	0.96
$In4d_{3/2}$ - InP_{ox}	20.0	0.68	19.9	0.96
$P2p_{3/2}$ - InP	128.5	0.70	128.6	1.02
$P2p_{1/2}$ - InP	129.4	0.70	129.5	1.02
$P2p_{3/2}$ - InP_{ox}	133.0	0.70	133.0	1.02
$P2p_{1/2}$ - InP_{ox}	133.9	0.70	133.9	1.02

Regarding the quantitative aspect, interesting evolutions are also noticed. Indeed, In surface enrichment is evidenced through XPS measurements, with In/P ratios evolving from 1.00 ± 0.03 to 1.40 ± 0.03 (Table 2). This suggests that when stopping the RF plasma sputtering process In metallic sites are created at the surface and some P (lighter) is preferentially released. This is only inherent to the process stop since no preferential sputtering is observed during dynamic profiling (Fig. 1).

As observed on Fig. 3 b. and c., after GD-OES sputtering, the crater surface has a specific morphology compared to a pristine InP surface (Fig. 3 a). Two types of defects are observed. First, (labeled 1 on Fig. 3 b. and enlarged in Fig. 3 c.) small balls of 10 to 20 µm diameter appear inside the crater. Secondly, the roughness is modified (labeled 2 on Fig. 3 b.) inside the GD-OES crater, with the presence of small circular impacts, randomly distributed

everywhere. The composition determined by XPS is averaged over 400 µm and therefore does not enable to separate the contributions of this heterogeneous surface.

Complementary EDS measurements (interaction volume around 1µm) informs at a higher lateral resolution but deeper in the volume. Those results (Table 2) confirm the In enrichment, with a ratio up to 1.81 ± 0.03 on the balls and ratio of 1.02 ± 0.03 outside the balls coherent with the InP matrix. Thus, In enrichment can be attributed to the presence of such balls, explaining also the XPS In/P ratio of 1.40. This is also confirmed by local characterization using Auger nano-probe showing a higher In content on the balls but also that the balls are not only composed of metallic In as the In-MNN Auger fingerprint, different from the InP one, is nevertheless not perfectly similar to the In metallic one[18] (Fig. 2 c.).

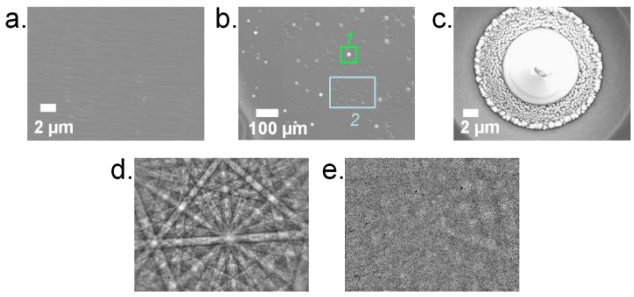

FIG. 3. SEM images of InP surface (a.), GD-OES crater (b.), In metallic ball inside the GD-OES crater (c.) and EBSD Kikuchi patterns for InP surface (d.) and GD-OES crater (e.).

Fig. 3 d. and e. show the EBSD results and the evolution of the Kikuchi patterns for an InP surface before and after GD-OES sputtering. The disappearance of such patterns after the sputtering (Fig. 3 e.) is another proof of the surface amorphization.

TABLE 2. Comparison of In/P ratio with two quantitative techniques: XPS and EDS (measured at 10 kV).

Ratios	InP surface		GD-OES crater		
	XPS	EDX	XPS	EDX	
				Ball	Outside
In/P	1.00	0.96	1.40	1.81	1.02

2. *Optical modifications*

SE is an excellent tool to assess the different perturbations induced by the GD-OES interruption. Firstly, our experiments have shown that SE measurements are perfectly repeatable inside the GD-OES crater, whatever the profiling duration performed, demonstrating that the final surface evolution at the end of the plasma sequence is the same regardless the depth reached by the profiling sequence. It is a post RF plasma etching steady state.

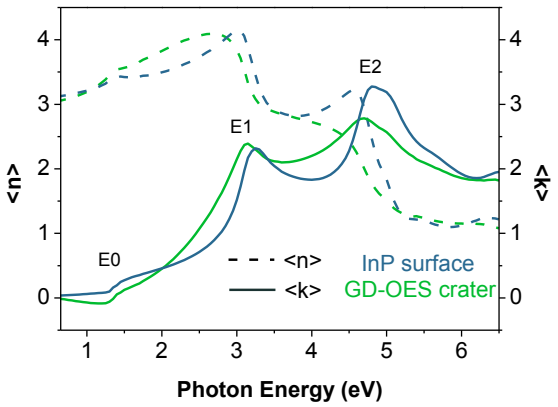

FIG. 4. Optical indexes (<n> and <k>) of InP deoxidized surface (blue) and GD-OES crater surfaces (green).

Optical indexes <n> and <k> evolutions between freshly deoxidized InP unperturbed surface and GD-OES crater bottom are displayed in Fig. 4. The optical indexes of deoxidized InP surface are in good agreement with literature[19]. After GD-OES plasma stop, modifications all over the energy range are shown, with an apparent position shift to lower energy values for E1 and E2 transitions (respectively from 3.25 eV to 3.1 eV and 4.8 eV to 4.65 eV). We also note a negative pseudo <k> for the energy under the InP band gap value. It could be explained by a refractive index of the top layer higher than the InP substrate one, which is confirmed by modeling (respectively at E=0.85eV, the effective refractive index of the top layer is 3.96 versus 3.17 for the InP substrate one).

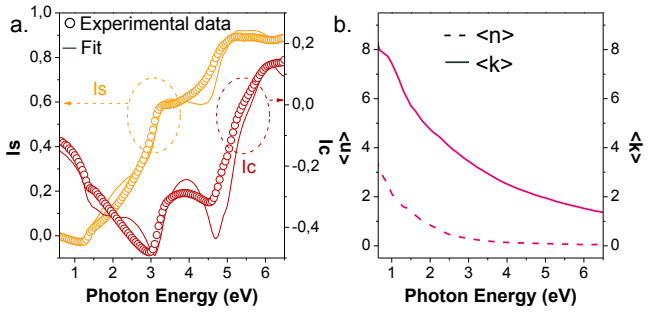

FIG. 5. Fit Results (Is, Ic)=f (E) obtained for the GD-OES crater surface, with Is = sin2ψ.sin Δ and Ic = sin 2ψ cos Δ (a.) and optical indexes <n> and <k> for metallic In (b.).

The attempt of SE modeling inside the crater is performed in Fig. 5 a., with a Maxwell Garnet Effective Medium Approximation[20], in consistency with SEM images showing small quantities of In balls at the surface, and then, an inhomogeneous surface. This model of Is = sin2ψ.sin Δ and Ic = sin 2ψ.cos Δ, presents the advantage to perform better simulations in this case than the effective medium approximation one, especially at low energy range. The proposed model is a one layer model on a deoxidized InP substrate. The layer is described by a mixture of two components to take account for the roughness observed at the surface: metallic In (for the In balls) and InP substrate. No voids are used here as the In enriched balls

are considered inside the InP substrate and not placed on top of the surface. Regarding metallic In, as far as we know, only few publications deal with SE[21]. We then have determined our proper value using SE measurement performed on a pure In ingot, beforehand dipped in 6 M HCl solution to prepare the surface. The deduced optical indexes <n> and <k> are shown in Fig. 5 b. Note that they are in reasonable agreement with the literature ones[21].

The performed modeling results (Fig. 5 a.) present two areas of interest. The first one is the sub band gap area (photon energy <1.34 eV), with a good agreement between modeled and experimental data, especially for Is. The second one, regarding the E1 and E2 transitions where values do not converge. This can be easily explained by the different components that were considered inside our model. Indeed, combination of metallic In and InP substrate in the over-layer contribution is a too simple approximation. While a metallic In component is perfectly justified, a more appropriate choice to model the external InP component has to be considered. Obviously the external InP is perturbed and this perturbation must be considered optically. XPS measurements clearly display that the chemical response of InP is modified. The loss of the spin orbit splitting of the P2p level is a clear indication that the perturbation of the outer part of the InP layer has to be considered. A suitable model to take account of this apparent surface amorphization is in progress, even if our first approximation of the order of magnitude inserted inside the model is in good agreement with the one observed in XPS (few nm). Indeed, the SE modeling result shows a thickness layer of 4.4 nm with a volume fraction of 12% metallic In and 88% InP substrate. Ratios between metallic In and InP substrate are also in good agreement with the SEM observation (Fig. 3 b.) showing the presence of random In metal balls at the surface.

Note that the notion of superficial perturbation agrees with additional Photoluminescence (PL) measurements. Actually, when the laser is pointed on an InP image zone without In ball, the PL signal decays in the crater by a factor of 5 which is consistent

with an ultra-thin superficial PL dead layer. However it is important to point out that all optical responses, and particularly the SE one, agree with a complex situation mixing metallic In screening site, InP modified thin layer and InP unperturbed substrate.

B. Regeneration with nanometer scale surface dissolution

The presence of a perturbation layer at InP surface inside the crater has been evidenced and fully characterized. The recovery of the initial properties of the semi-conductor is possible through different techniques, among them nano-chemical engineering. This intermediary step is therefore mandatory to validate the sequential analyses operated by GD-OES and XPS coupling. The resulting surface is presented using not only XPS but also SE, who has proved to be an efficient tool for such surface problematic.

1. Chemical regeneration

Several chemical treatments can be applied in order to succeed to perform a nano-chemical regeneration[18]. However, depending on the nature of the studied semi-conductor, the formulation has to be adapted. The first attempt to retrieve the chemical information was performed through a dipping in HCl 2 $mol.L^{-1}$ during 2 minutes, as this is known to be a good InP deoxidation can be achieved in HCl[22]. However, as observed on Fig. 6 (semi-regenerated crater), the chemical treatment is not sufficient to obtain a total regeneration, as for P2p and In4d the spin orbit splitting is not fully recovered, the FWHM broadening still visible and the surface not deoxidized. One of the different options considered to improve this chemical treatment is to modify the dipping duration. By conserving the same HCl concentration, the immersion time is prolonged up to 15 minutes. In this case, at the XPS scale a perfect regeneration of the chemical environment is shown with the reemergence of both photopeaks

spin orbit splitting is clearly visible (Fig. 6, regenerated crater) as well as a narrowing of the FWHM parameters (0.65 ± 0.05 for P2p and 0.66 ± 0.05 eV for In4d).

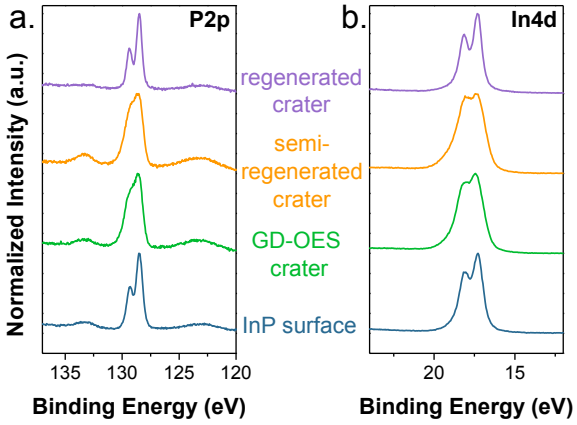

FIG. 6. XPS high energy resolution spectra of P2p (a.) and In4d (b.) photopeaks obtained on InP for an unperturbed surface (blue) and inside the GD-OES crater before (green) and after chemical regeneration in HCl 2 mol.L^{-1} 2 min (yellow) and 15 min (purple).

After the 15min treatment, the surface morphology and crystalline properties are similar to the one presented Fig 3 a. for bare deoxidized InP substrate. In-rich balls have totally disappeared. This is consistent with the photopeaks fingerprints presenting well defined doublets and the In/P XPS ratio of 1.02 ± 0.03 as expected for a pristine homogeneous InP surface.

2. Optical regeneration

In Fig. 7, the optical indexes evolutions are displayed in function of the chemical treatment regeneration. Similar trends are observed between the recovery of the optical parameter and the chemical ones presented in the previous paragraph. After the short immersion time (2 min dipping in HCl), this intermediate step of regeneration is not sufficient to completely remove the perturbation induced at the end of GD-OES sequence. However,

once a 15 minutes dipping is performed, the optical indexes <n> and <k> are similar to the initial InP pristine substrate, bringing evidence of a renewed InP surface.

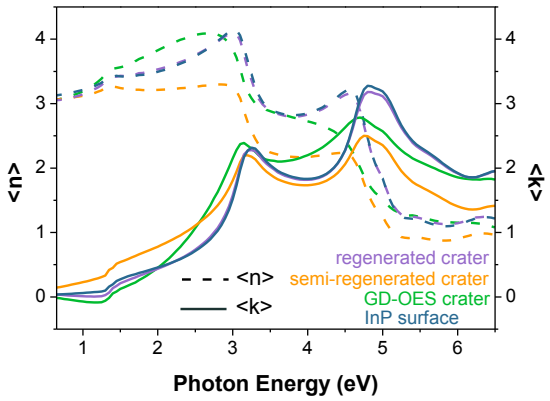

FIG. 7. Optical indexes (<n> and <k>) of pristine InP (blue) and GD-OES crater surfaces before (green) and after chemical regeneration in HCl 2 mol.L^{-1} 2 min (yellow) and 15 min (purple).

Note that using the semi-regenerated crater experimental data, the quality of the GD-OES crater bottom SE signal modeling can be improved by, especially within the high energy range.

IV. SUMMARY AND CONCLUSIONS

By combining mainly SE and XPS characterizations, assisted by other techniques such as SEM, EDS, EBSD, Auger and PL measurements, we show that a complete evaluation of the chemical and optical modification of an InP surface after the interruption of a RF Argon plasma / InP surface interaction can be performed. The first important result pointed out in this work is that whatever the etching time the plasma leaves similar final surface states. This surface is specific of the plasma surface interaction and the GD-OES stop configuration and reproducible from one InP sample to another. The interest of combining XPS and SE

characterization tools is their total complementarity bringing an accurate diagnosis of the surface modification nature, structuration and organization. Both XPS and SE results suggest that a very thin external surface layer is present but, in both cases, with a part of the responses linked to the InP substrate contribution. On one hand, XPS demonstrates that the surface is In rich, amorphous, present a new metallic component in relation with its specific morphology. On the other hand, SE response is also consequently modified but clearly conserves an InP trend and component for the signal modelling. So, one should consider the combination of a surface layer and a substrate response to describe surface inside the crater. Such observations suggest that the surface layer is thin (few nanometers) and inhomogeneous in agreement with SEM observations evidencing heterogeneities at the surface.

This inhomogeneity is a strong challenge for the SE interpretation but also for the XPS one. Concerning the attempt to model the characteristic SE responses, it is evident that our simple proposition of a combined over layer constituted by a metallic In and an InP contributions is not enough to provide an optimal simulation. To increase the pertinence of this approach, we think that optical constant of the outer InP would be slightly different from the perfect substrate one. The specificity of the In4d and P2p photopeaks, with broadened FWHM and subsequent spin orbit splitting loss suggests, in agreement with EBSD characterization showing the disappearance of the Kikuchi patterns, that the outer InP layer is different. So, a specific model for this outer InP contribution has to be developed. Nevertheless, present results clearly evidence that the qualitative comparison of the SE response is sufficient to determine if a surface chemical modification has occurred. SE is a very efficient technique to follow by a non-destructive way and in reasonable acquisition time the variations of the optical response in relation with variation of experimental conditions. SE is easier to perform than systematic XPS characterization and offer as for XPS, the possibility to perform mapping. Going back to the present context, dealing with GD-OES and XPS

coupling, the last point demonstrated in this paper is the SE capability to be a privileged tool to evaluate not only the perturbation but also the regeneration of the surface. In this work, regeneration was performed ex situ using a wet chemical treatment and characterized ex situ as well. A fine optimization of this procedure can be envisaged by performing SE in a liquid cell (mainly used for kinetic purpose) containing the sample immersed, and bringing in situ surface evolution.

ACKNOWLEDGMENTS

This work was carried out in the framework of IPVF. This project has been supported by the French Government in the frame of the program of investment for the future (Programme d'Investissement d'Avenir – ANR-IEED-002-01).

[1] F.J. Grunthaner, P.J. Grunthaner, R.P. Vasquez, B.F. Lewis, J. Maserjian, and A. Madhukar, J. Vac. Sci. Technol. **16**, 1443 (1979).

[2] S.P. Kowalczyk, E.A. Kraut, J.R. Waldrop, and R.W. Grant, J. Vac. Sci. Technol. **21**, 482 (1982).

[3] E. Scalise, V. Srivastava, E. Janke, D. Talapin, G. Galli, and S. Wippermann, Nat. Nanotechnol. **13**, 841 (2018).

[4] D. Mercier, M. Bouttemy, J. Vigneron, P. Chapon, and A. Etcheberry, Appl. Surf. Sci. **347**, 799 (2015).

[5] H. Fujiwara, *Spectroscopic Ellipsometry : Principles and Applications* (John Wiley & Sons, 2007).

[6] A. Gagnaire, J. Joseph, A. Etcheberry, and J. Gautron, J. Electrochem. Soc. **132**, 1655 (1985).

[7] A. Gagnaire, J. Joseph, and A. Etcheberry, J. Electrochem. Soc. **134**, 2475 (1987).

[8] A. Loubat, C. Eypert, F. Mollica, M. Bouttemy, N. Naghavi, D. Lincot, and A. Etcheberry, Appl. Surf. Sci. **421**, 643 (2017).

[9] A.J. Barlow, N. Sano, B.J. Murdoch, J.F. Portoles, P.J. Pigram, and P.J. Cumpson, Appl. Surf. Sci. **459**, 678 (2018).

[10] D.E. Aspnes and A.A. Studna, Phys. Rev. B **27**, 985 (1983).

[11] P. Lautenschlager, M. Garriga, and M. Cardona, Phys. Rev. B **36**, 4813 (1987).

[12] S. Adachi, Phys. Rev. B **35**, 7454 (1987).

[13] C.M. Herzinger, P.G. Snyder, B. Johs, and J.A. Woollam, J. Appl. Phys. **77**, 1715 (1995).

[14] I. Subedi, M.A. Slocum, D. V. Forbes, S.M. Hubbard, and N.J. Podraza, Appl. Surf. Sci. **421**, 813 (2017).

[15] S. Gaiaschi, S. Richard, P. Chapon, and O. Acher, J. Anal. At. Spectrom. **32**, 1798 (2017).

[16] A. Loubat, S. Bechu, M. Bouttemy, C. Eypert, S. Gaiaschi, M. Fregnaux, D. Aureau, J. Vigneron, N. Simon, P. Chapon, A.-M. Goncalves, and A. Etcheberry, in *2018 IEEE 7th World Conf. Photovolt. Energy Convers. (A Jt. Conf. 45th IEEE PVSC, 28th PVSEC 34th EU PVSEC)* (IEEE, 2018), pp. 0066–0070.

[17] D. Aureau, M. Frégnaux, M. Bouttemy, J. Vigneron, N. Simon, A. Etcheberry, and A.-M. Gonçalves, Meet. Abstr. **MA2019-01**, 1213 (2019).

[18] A.C. Parry-Jones, P. Weightman, and P.T. Andrews, J. Phys. C Solid State Phys. **12**, 1587 (1979).

[19] C.M. Herzinger, P.G. Snyder, B. Johs, and J.A. Woollam, J. Appl. Phys. **77**, 1715 (1995).

[20] J.C. Garnett Maxwell, Philos. Trans. R. Soc. London Ser. A **203**, 385 (1904).

[21] R.Y. Koyama, N. V. Smith, and W.E. Spicer, Phys. Rev. B **8**, 2426 (1973).

[22] R. Vos, S. Arnauts, T. Conard, A. Moussa, H. Struyf, and P.W. Mertens, Solid State Phenom. **187**, 27 (2012).